YALE
PEABODY
MUSEUM

P.O. BOX 208118 | NEW HAVEN CT 06520-8118 USA | PEABODY.YALE. EDU

JOURNAL OF MARINE RESEARCH

The *Journal of Marine Research,* one of the oldest journals in American marine science, published important peer-reviewed original research on a broad array of topics in physical, biological, and chemical oceanography vital to the academic oceanographic community in the long and rich tradition of the Sears Foundation for Marine Research at Yale University.

An archive of all issues from 1937 to 2021 (Volume 1–79) are available through EliScholar, a digital platform for scholarly publishing provided by Yale University Library at https://elischolar.library.yale.edu/.

Requests for permission to clear rights for use of this content should be directed to the authors, their estates, or other representatives. The *Journal of Marine Research* has no contact information beyond the affiliations listed in the published articles. We ask that you provide attribution to the *Journal of Marine Research*.

Yale University provides access to these materials for educational and research purposes only. Copyright or other proprietary rights to content contained in this document may be held by individuals or entities other than, or in addition to, Yale University. You are solely responsible for determining the ownership of the copyright, and for obtaining permission for your intended use. Yale University makes no warranty that your distribution, reproduction, or other use of these materials will not infringe the rights of third parties.

This work is licensed under a Creative Commons Attribution-NonCommercial-ShareAlike 4.0 International License.
https://creativecommons.org/licenses/by-nc-sa/4.0/

Journal of Marine Research, 66, 191–218, 2008

Modeling effects of patchiness and biological variability on transport rates within bioturbated sediments

by Sebastien Delmotte[1,2], Magali Gerino[3], Jean Marc Thebault[3] and Filip J. R. Meysman[4]

ABSTRACT

Bioturbation models are typically one-dimensional, with the underlying assumption that tracer gradients are predominantly vertical, and that sediment reworking is laterally homogeneous. These models implicitly assume that bioturbation activity does not vary with horizontal location on the sediment surface. Benthic organisms, however, are often patchily distributed. Moreover, due to natural variability, bioturbation activity varies among individuals within a population, and hence, among bioturbated patches. Here we analyze a 1D model formulation that explicitly includes patchiness, exemplified by conveyor-belt transport. The patchiness is represented with one coefficient α_b, as the fraction of bioturbated areas of the total area. First, all the mixed patches are considered to feature the same bioturbation rates. Then variability of these rates among patches is introduced in the model. The model is analyzed through different scenarios to assess the influence of patchiness and biological variability on the resulting tracer profiles (luminophores, ^{234}Th and ^{210}Pb). With patchiness, the principal feature of the resulting profiles is exponential decrease of tracer concentrations near the SWI, due to the accumulation of particles in the nonbioturbated patches, and the presence of subsurface peaks or anomalous concentrations at depth, as the result of particle transport in the bioturbated patches. This pattern is unusual compared to published patterns for conveyor-belt transport. Adding intra-population variability in bioturbation rates induces biodiffusive-like transport, especially with luminophores. This theoretical work provides new insights about the influence of patch structure on particle dispersion within sediments and proposes a new applicable approach to model various bioturbation processes (type and rates of transport) that can be horizontally distributed in sediments.

1. Introduction

Bioturbation is defined, in its strict sense, as the transport of particles within the sediment resulting from the reworking by the benthic organisms (Meysman *et al.,* 2006). The quantification of bioturbation is classically based on the analysis of vertical tracer

1. MAD-Environment (Modeling and Analysis of Data in Environment), Allée des Demoiselles, 33170 Gradignan, France.
2. Corresponding author. ***email: delmotte@mad-environnement.com***
3. Ecolab, UMR CNRS UPS 5245, Université Toulouse 3, 29 rue Jeanne Marvig, 31055 Toulouse Cedex 04, France.
4. Department of Analytical and Environmental Chemistry, Vrije Universiteit Brussel (VUB), Pleinlaan 2, B-1050 Brussels, Belgium.

profiles measured in sediment cores. The application of suitable transport models to these tracer profiles then provides an estimate of the intensity of bioturbation, usually expressed in the form of a biodiffusion coefficient D_b. Such biodiffusive models were first introduced as empirical descriptions several decades ago (Goldberg and Koide, 1962), and afterwards, supported by theoretical arguments, as in Guinasso and Schink (1975), Berner (1980), Boudreau (1986a,b) and Meysman *et al.* (2003). However, the simplifying assumptions underlying the biodiffusion model are sometimes violated, particularly for short-lived tracers (Meysman *et al.,* 2003; Reed *et al.,* 2006). For these cases, more complex descriptions have been proposed, such as the nonlocal exchange formulation (e.g. Boudreau and Imboden, 1987) or head-down deposit-feeding models (Fisher *et al.,* 1980; Robbins, 1986; Rice, 1986; Delmotte *et al.,* 2007).

A common feature of all these bioturbation models (whether biodiffusive or nonlocal) is that they are one-dimensional. Hence, the underlying assumption is that tracer gradients are predominantly vertical, and sediment reworking is laterally homogeneous. In other words, when viewed from above, all sediment areas are assumed to be affected in exactly the same way. It is well known, however, that benthos assemblages often show spatial zonation and patchiness in sediments (e.g. Aller, 1982; Thrush, 1991). Current models do not account for such horizontal heterogeneity in the distribution of organisms, which could induce patchy reworking, affecting nearby sediment areas in different ways. Here our aim is to investigate whether and when such patchy reworking can influence the analysis of tracer profiles from sediment cores.

Spatial heterogeneity in the distribution of bioturbating fauna results from a number of factors (Peterson, 1991; Hewitt *et al.,* 1997). First, direct biological interactions, such as predation, competition, reproduction and larval settlement, are spatially dependent, and hence, they will influence the local population density of bioturbating fauna (Kneib, 1984; Commito *et al.,* 1995; Lindsay *et al.,* 1996; Honkoop *et al.,* 2006). Second, variation in physical factors, such as flow patterns in the overlying water or gradients in sediment characteristics, also contribute to zonation and patchiness (Gray, 1974; Kneib, 1984; Levinton and Kelaher, 2004). Finally, the modification of sediment properties by bioturbation can also facilitate (Commito *et al.,* 1995) or prevent (Aller and Dodge, 1974) the settlement of other species. Clearly, the notion of spatial heterogeneity is dependent on the scale of observation. Gradients in the abundance and biomass of bioturbating fauna can range from the mm-scale of the organisms (Maire *et al.,* 2007) to the km-scale of the depositional facies (Aller and Dodge, 1974). The spatial structure within the fauna assemblages follows a nested hierarchy, resulting from the influence of physical processes that operate at large scales and biological factors that operate at smaller scales (Thrush *et al.,* 1997).

A direct consequence of heterogeneity in the spatial distribution of fauna is the concomitant variation of sediment reworking. Reworking rates may vary because certain bioturbators are either present or absent at a particular location. Moreover, the intensity of bioturbating activity may also vary among individuals within a population, providing an

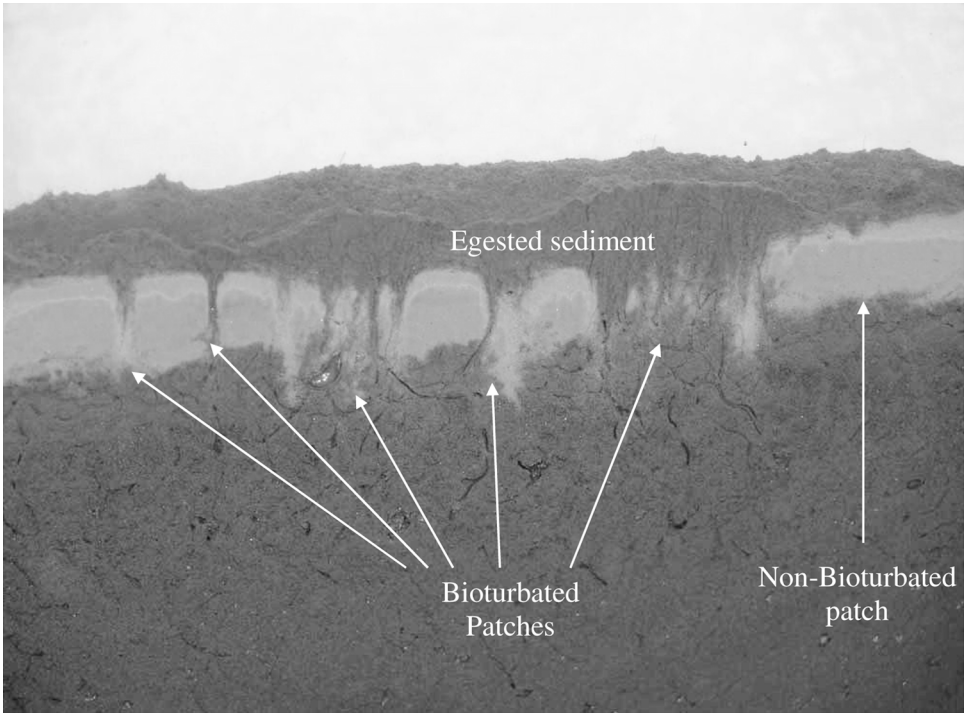

Figure 1. Photograph showing the 2D distribution of luminophores (light gray) in a sediment (dark gray) inhabited by tubificid oligochaetes (50 000 ind. m^{-2}), 11 days after the deposition of the tracers at the sediment-water interface (A. Ciutat, pers. comm.). The patchy reworking of the sediment is apparent: well-mixed zones alternate with zones where the tracer layer remains undisturbed. The presence of egested sediment over the tracer layer in the bioturbated zones illustrates the conveyor-belt transport. The displayed sediment domain is about 10 cm wide × 6 cm deep. The total surface area of the microcosm (seen from above) was about 30 cm^2.

additional source of spatial heterogeneity in sediment reworking (Aller, 1982). The spatial scale at which bioturbation varies can be smaller than the diameter of the sediment core taken, but may be as large as at the scale of a depositional basin (Aller *et al.,* 1980). A bioturbated patch at large scale (10^2 m or greater) could be defined as an area where the mixing processes are roughly homogeneous because it is inhabited by the same benthic community and it shows similar physico-chemical properties. At meso- and small-scale (1 to 10^2 m), even if the sediments characteristics are apparently homogeneous, the distribution of organisms can be heterogeneous (e.g. Parry *et al.,* 2003), and hence bioturbation processes may locally vary. Finally, bioturbation can be patchy at the micro-scale (10^{-3} to 1 m): indeed, depending on the density, the size and the behavior of the organisms, sediment mixing can occur on few centimeters around the location of the organism(s) whereas the surrounding sediment is not bioturbated. Figure 1 provides a good illustration of the micro-scale heterogeneity of sediment reworking by oligochaete tubificids (A.

Ciutat, pers. comm.). Bioturbation models are also applied at these very different scales, e.g., at the micro-scale, to quantify the faunal reworking activity within a single sediment core as is done in tracer analysis, and also at the large-scale, to model the biogeochemical functioning of the sediment at the scale of the whole lake, the estuary or even the global ocean (e.g., Archer *et al.,* 2002).

Up to the present, the patchy reworking of sediments and its implications for bioturbation modeling have not been examined in detail. Wheatcroft *et al.* (1990), Mohanty *et al.* (1998) and Timmermann *et al.* (2003) explored models which allowed lateral heterogeneity in bioturbation processes, but these studies did not systematically examine the influence of patchiness on tracer profiles. François *et al.* (1997, 2001, 2002) have developed 2D models that can be used to simulate a patchy reworking, but the 1D counterparts of these models were not investigated. Here, we present an analysis of patchiness in the 1D models of bioturbation, based on the conveyor-belt transport of tubificid worms, which are often dominant bioturbators in freshwater sediments. Tracer dispersion by conveyor-belt deposit feeders has been described and modeled by several authors in the past (Fisher *et al.,* 1980; Robbins, 1986; Rice, 1986; Delmotte *et al.,* 2007). Here, a generalization of this model approach is developed that accounts for patchy reworking and the variation of biological activity within different patches. The effects of patchiness and biological variability are then investigated for tracer experiments (luminophores, short-lived and long-lived radioisotopes) that are classically used in bioturbation research.

2. Model development

a. Model for a uniformly reworked sediment

In a first model, we assume that there is no lateral variability in bioturbation activity, so the whole sediment surface is uniformly reworked. This will serve as a baseline model to compare other scenarios. Our model focuses on one specific type of bioturbation activity: conveyor-belt deposit feeding by tubificid oligochaetes. This conveyor-belt bioturbation model was recently analyzed in detail by Delmotte *et al.* (2007) and forms an adaptation of the classical conveyor-belt models presented in Fisher *et al.* (1980), Robbins (1986), and Rice (1986). For a solid tracer that is not subject to chemical reactions, the time-dependent mass conservation equation becomes

$$\frac{\partial C}{\partial t} = \frac{\partial}{\partial z}\left[(D_b(z) + D_{nb}) \frac{\partial C}{\partial z} \right] - \frac{\partial}{\partial z}[\omega_b(z)C] - k_b(z)C - \lambda C \qquad (1)$$

where z represents the depth into the sediment (cm), t is time (yr) and C is the tracer concentration (mg g^{-1} of dry sediment). The mass balance (1) is a classical diffusion-advection-reaction equation. For simplicity, we assume that porosity remains constant with depth, so that porosity terms do not feature in this mass balance (Meysman *et al.,* 2005). The parameter λ represents the decay rate of the radiotracer. The diffusion coefficient D_{nb} ($cm^2\ yr^{-1}$) represents the rate of particle mixing due to purely physical processes

(erosion-resuspension, wave action, etc). The other parameters with subscript "b" describe the biological transport induced by the deposit-feeding tubificids. This transport is modeled as a superposition of two effects: (i) a conveyor-belt mechanism, where the sink coefficient k_b models the ingestion of particles at depth, and the bioadvective velocity ω_b (cm yr^{-1}) models the resulting downward transport of sediment; and (ii) a small-scale mixing mechanism that represents particle reworking activities other than deposit feeding (e.g., burrow contraction, vertical movements between the depth and the surface, locomotion at the sediment surface). This small-scale mixing is represented by the biodiffusion coefficient D_b. Biodiffusion is made depth dependent because it is typically present only in the first centimeters of the sediment (Aller, 1982). It decreases with depth according to the relation:

$$D_b(z) = D_b^0 \exp\left[-\frac{1}{2}\left(\frac{x}{x_{mix}}\right)^2\right] \tag{2}$$

where D_b^0 is the mixing intensity at the sediment-water interface (cm^2 yr^{-1}), and the attenuation coefficient x_{mix} represents a characteristic mixing depth (cm). Note that the tracer profiles have been shown to be relatively insensitive to such small-scale mixing in the case of conveyor-belt transport (Rice, 1986; Delmotte *et al.,* 2007).

The ingestion rate is dependent on depth, and is modeled by the Gaussian function:

$$k_b(z) = k_{ing}^{\max} \exp\left[\frac{(z - z_{ing})^2}{2\sigma_{ing}^2}\right] \tag{3}$$

where $k_{ing}^{\max}$ is the maximal ingestion rate (yr^{-1}), z_{ing} is the mean depth where organisms are deposit feeding (cm), and σ_{ing} is the square root of the variance of this ingestion depth (cm). The ingestion relation (2) can be justified if we assume that the population of conveyor-belt organisms has a normal size distribution, and the size of the organisms linearly scales with the depth at which they feed (Delmotte *et al.,* 2007). Downward bioadvection is a consequence of the removal of sediment at depth by conveyor-belt deposit feeding. The bioadvective velocity is not an independent parameter of the model, but is constrained by the mass balance for the bulk sediment (Boudreau, 1997; Delmotte *et al.,* 2007)

$$\omega_b(z) = \int_z^L k_b(u)du \tag{4}$$

where L represents the depth of the model domain (cm).

b. Model for a patchily reworked sediment

In a second model, we assume that the sediment is reworked in patches where the sizes of these patches are smaller than that of the core. The fraction α_b represents the fraction of the sediment surface that is reworked ($0 \leq \alpha_b \leq 1$). We assume that all patches are

similarly reworked, and that within a patch, the same bioturbation activity is occurring as in the uniformly reworked scenario. Moreover, we assume that the patchiness remains steady in time. By this we mean that over the time scale of the tracer experiment, the macrofauna will remain within their patch, and will not colonize new patches. The validity of this assumption clearly depends on the reactivity (half-life) of tracers that are used, and on the mobility of the bioturbating fauna. For short experiments (luminophores, short-lived radiotracers) this assumption seems justifiable. However, for long-lived radiotracers (e.g. ^{210}Pb) the assumption will in general not be valid (note that we will still carry out some simulations for ^{210}Pb to enable a comparison with the short time-scale tracers).

To arrive at a consistent model, we must derive separate model equations for bioturbated and nonbioturbated patches. The transport of solid tracers within a reworked patch is given by

$$\frac{\partial C_b}{\partial t} = \frac{\partial}{\partial z}\left[(D_b(z) + D_{nb}) \frac{\partial C_b}{\partial z} \right] - \frac{\partial}{\partial z}\left[\omega_b(z) C_b\right] - k_b(z) C_b - \lambda C_b \tag{5}$$

where C_b now denotes the solid concentration within a bioturbated patch. This equation is exactly the same as (1), except for a change of the concentration from C to C_b. The nonbioturbated patches take up a fraction $\alpha_{nb} = 1 - \alpha_b$ of the sediment, and are only subject to the background physical mixing

$$\frac{\partial C_{nb}}{\partial t} = D_{nb} \frac{\partial^2 C_{nb}}{\partial z^2} - \lambda C_{nb} \tag{6}$$

The symbol C_{nb} now represents the tracer concentration within a nonbioturbated patch.

When taking cores within a patchily bioturbated sediment, the resulting "averaged" tracer distribution would reflect a mix of the bioturbated and nonbioturbated areas that were captured by coring. If we assume that the coring process is random (no bias occurs when selecting the areas that are included in cores), the expected "average" concentration within a sediment core at a given depth is

$$C = \alpha_b C_b + \alpha_{nb} C_{nb} \tag{7}$$

Assuming that each patch is independently affected, we can make a linear combination of the conservation Eqs. (5) and (6) for the respective bioturbated and nonbioturbated patches. The resulting "averaged" mass balance for the evolution of the tracer within a core thus becomes

$$\begin{aligned} \frac{\partial\{\alpha_{nb} C_{nb} + \alpha_b C_b\}}{\partial t} = \alpha_{nb}\left\{ D_{nb} \frac{\partial^2 C_{nb}}{\partial z^2} - \lambda C_{nb} \right\} + \alpha_b \Bigg\{ \frac{\partial}{\partial z}\left[(D_b(z) + D_{nb}) \frac{\partial C_b}{\partial z} \right] \\ - \frac{\partial}{\partial z}\left[\omega_b(z) C_b\right] - k_b(z) C_b - \lambda C_b \Bigg\} \end{aligned} \tag{8}$$

This equation can be further rearranged to

$$\frac{\partial C}{\partial t} = \left\{ D_{nb} \frac{\partial^2 C}{\partial z^2} - \lambda C \right\} + \alpha_b \left\{ \frac{\partial}{\partial z} \left[D_b(z) \frac{\partial C_b}{\partial z} \right] - \frac{\partial}{\partial z} [\omega_b(z) C_b] - k_b(z) C_b \right\} \quad (9)$$

Eq. (9) has not been used in modeling studies, and is the focus of our model analysis here. It includes both the variables C and C_b, and thus, it is not a complete model statement in itself. One needs to simultaneously solve Eq. (5) in order to calculate the concentration C_b.

Eq. (9) can be regarded as an extension of the original model (1). If $\alpha_b = 0$, then Eq. (9) reduces to the "abiotic" diffusion model described by Eq. (6). If $\alpha_b = 1$, Eq. (9) reduces to the conventional conveyor-belt model presented in Eq. (1). Between these two end members, Eq.(9) produces the average concentration profile for a solid tracer in a patchily bioturbated sediment.

c. Biological variability: n patch types with different transport rates

In a third model, we assume that the bioturbated area is composed of n different types of patches in which the transport rates (ω_b and k_b) are different. The underlying idea is that natural variation in the size of individuals within a population results in various depth of ingestion and bio-advective velocities, as underlined by Aller (1982). Eq. (9) can be readily generalized to

$$\frac{\partial C}{\partial t} = \left\{ D_{nb} \frac{\partial^2 C}{\partial z^2} - \lambda C \right\} + \sum_{i=1}^{n} \alpha_{b,i} \left\{ \frac{\partial}{\partial z} \left[D_b(z) \frac{\partial C_{b,i}}{\partial z} \right] - \frac{\partial}{\partial z} [\omega_{b,i}(z) C_{b,i}] - k_{b,i}(z) C_{b,i} \right\} \quad (10)$$

where $C_{b,i}$ represents the solid concentration in the ith patch type, $k_{b,i}$ denotes the ingestion rate in the ith patch type, $\omega_{b,i}$ is the subsequent bioadvection velocity in the ith patch and $\alpha_{b,i}$ is the area fraction of the ith patch type. The ingestion rate is specified in the same way as in Eq. (3) by the Gaussian function:

$$k_{b,i} = k_{ing,i}^{\max} \exp\left[\frac{(z - z_{ing})^2}{2\sigma_{ing}^2} \right] \quad (11)$$

where $k_{ing,i}^{\max}$ is the maximal ingestion rate (yr^{-1}) in the ith patch type. We assume that only the maximal ingestion rate differs between patches (z_{ing} and σ_{ing} are kept constant). The subsequent bioadvective velocity $\omega_{b,i}$ is calculated via Eq. (4). As noted previously, D_b is not a major feature of conveyor-belt transport, and so it is set constant among the n patches to keep the model simple. When there is only a single type of patch (n = 1), Eq. (10) readily reduces to Eq. (9).

d. Boundary conditions

We ran the above models with two types of boundary conditions at the sediment-water interface (SWI). First, we simulated the deposition of a thin layer of solid tracer on the SWI at $t = 0$ and followed the downward mixing of this "pulse," as observed in luminophore

experiments (Robbins, 1986; Gerino *et al.,* 1998; Ciutat *et al.,* 2005a, b; Fernandes *et al.,* 2006). The initial condition is idealized as a Dirac delta function at the SWI, and during the simulation, both the upper and lower model boundaries are modeled as impenetrable (no-flux condition). In a second case, we consider a constant external supply of particle-bound radioisotopes at the SWI. The input of particles entering the ith bioturbated patch is governed by the flux condition

$$F_i^b(t) = -\rho(1-\varphi)D_b(0)\left.\frac{\partial C_{b,i}}{\partial z}\right|_{z=0} + \rho(1-\varphi)\omega_{b,i}(0)C_{b,i}(0) \tag{12}$$

where the F_i^b is the total solid flux (mg cm^{-2} yr^{-1}) that enters the patch. This flux is the sum of two components (Delmotte *et al.,* 2007)

$$F_i^b(t) = F_{eg,i}(t) + F_{ext}(t) \tag{13}$$

The flux F_{ext} represents the external supply at the SWI from overlying water. The biological component $F_{eg,i}$ results from particle egestion at the surface of the ith patch by the deposit feeders. The particles that are ingested at depth are deposited back at the SWI, and this input can be calculated as

$$F_{eg,i}(t) = \rho(1-\varphi)\int_0^L k_{b,i}(z)C_{b,i}(z,\,t)dz \tag{14}$$

where ρ is the density of the solid sediment (g cm^{-3}) and φ is the porosity. The solid flux F^{nb} entering the nonbioturbated patches is governed by the condition

$$F^{nb}(t) = -\rho(1-\varphi)D_{nb}\left.\frac{\partial C_{nb}}{\partial z}\right|_{z=0} \tag{15}$$

The biological flux vanishes in the nonbioturbated patches, so that

$$F^{nb}(t) = F_{ext}(t) \tag{16}$$

At the lower boundary, we assume a no-gradient condition in both scenarios

$$\left.\frac{\partial C}{\partial z}\right|_{z=L} = 0 \tag{17}$$

e. Numerical solution procedure

To obtain the solution to Eq. (9), we first solved Eq. (5) and Eq. (6) independently for the bioturbated and nonbioturbated patches and then calculated the average concentration profile using Eq. (7). The same method was employed to solve Eq. (10), where Eq. (5) was solved for individual patches with different transport rates. These simulations were then compared to the solution of the inconsistently averaged model (1). The simulations

presented here are all transient simulations performed in the FORTRAN90 programming language. In all simulations, Eq. (1), Eq. (5) and Eq. (6) were solved numerically using a Crank-Nicholson finite-differencing scheme. The time step was fixed at 1 min, and the spatial resolution was set to 0.01 cm. The accuracy and stability of the numerical solution were verified as in Delmotte *et al.* (2007), and the conservation of matter was checked. In the simulations of radioisotopes, steady state was said to be reached when the tracer profile no longer varied with time (the calculation stopped when, at each depth, the relative difference between the tracer concentrations on two consecutive days was lower than 10^{-4}).

3. Parameter values and simulation scenarios

a. Baseline parameter set

In all simulations, porosity φ was set to 0.8 and density ρ was fixed to 2.65 g cm^{-3}, representing a standard sediment environment. The height L of the modeled domain was 25 cm. Two particle-bound radioisotopes were simulated: ^{234}Th as a short-lived tracer ($t_{1/2}$ = 24.1 d, λ = 10.5 yr^{-1}) and ^{210}Pb as a long-lived tracer ($t_{1/2}$ = 22.3 yr, λ = 0.031 yr^{-1}). A constant input flux for these radioisotopes was imposed at the SWI.

Delmotte *et al.* (2007) suggested that tubificid bioturbation in freshwater sediments could be modeled via a generic parameter set that is representative across a wide range of environments. In all the simulations here, these values are used as the baseline parameter set. The small-scale diffusion coefficient D_b^0 was set to 3 cm^2 yr^{-1}, the characteristic depth x_{mix} was set to 2 cm, the depth of maximal ingestion z_{ing} was fixed at 5 cm, and the standard deviation of this ingestion depth σ_{ing} was set to 2 cm, following the analysis of tubificid bioturbation in Delmotte *et al.* (2007). The ingestion rate constant $k_{ing}^{\max}$ was set to 10 yr^{-1}. Given these values of $k_{ing}^{\max}$, z_{ing} and σ_{ing}, the resulting bioadvective velocity is about 50 cm yr^{-1} at $z = 0$. In the cases where the bioturbated area was composed of several patches that featured different ingestion rates: (i) all patch types were considered to be equally abundant, i.e., $\alpha_{b,i} = \alpha_b/n$; (ii) the value for ingestion rate $k_{ing,i}^{\max}$ in each patch was randomly attributed using a random-number generator (R software − function *rnorm*). Values for $k_{ing,i}^{\max}$ were chosen within the range 0–20 yr^{-1}, following a Gaussian distribution with a theoretical mean of 10 and a theoretical standard deviation of 2.5. For each sample of randomly generated values, the mean value was calculated as $\langle k_{ing}^{\max} \rangle = \frac{1}{n} \sum_i k_{ing,i}^{\max}$. To enable a proper comparison with the cases where all the bioturbated patches are similarly reworked, only sets of random values for which $\langle k_{ing}^{\max} \rangle = 10$ yr^{-1} were retained (Table 1). The abiotic mixing coefficient D_{nb} was set to a moderate background level of 0.1 cm^2 yr^{-1}, in order to be able to properly distinguish the effects of biological patchiness.

Table 1. Descriptive statistics of the values for maximal ingestion rate k_{ing}^{max} that were randomly allocated in the scenarios B and C. These sets of values ($n = 2$, 10 and 100) were randomly drawn from a Gaussian distribution with a mean of 10 yr^{-1} and a standard deviation of 2.5 yr^{-1} (R-software). To enable a proper comparison with the output from the scenario A, only the random sets that showed a mean of 10 yr^{-1} were retained.

	n = 2	n = 10	n = 100
Mean	10	10	10
Standard deviation	3.7	3.44	2.58
Median	10	10.8	9.9
Min-Max	7.4–12.6	3–14.3	3.9–17.7

b. Scenarios

i. Scenario A: Effects of patchiness. The effect of patchiness was examined by carrying out simulations for a range of α_b values. First, the two end-member values $\alpha_b = 0$ and $\alpha_b = 1$ were implemented, to respectively arrive at the purely abiotic mixing case and the uniformly bioturbated conditions. Then α_b values were set to 0.25, 0.5 and 0.75 to study different degrees of patchiness. The ingestion rate was taken constant over all bioturbated patches. Two types of tracer experiments were simulated as discussed above: (A1) A pulse input of conservative particles mimicking a typical experiment with luminophores under laboratory conditions. Transient solutions were calculated, and the downward migration of tracer is displayed at three time intervals (10, 50 and 100 d) spanning the transition from short-term to long-term mixing. (A2) A constant external input of particle-bound radioisotopes (^{234}Th and ^{210}Pb) to reproduce radiotracer profiles that are sampled in the field. Here, dynamic simulations were run until steady state. Profiles of tracer activity were normalized in such a way that new particles at the SWI had unit activity (Reed *et al.,* 2006).

As conventionally done in the analysis of radio-tracer profiles, a diffusive model solution [from Eq. (6)] was fitted to these model-generated radioisotope profiles in order to estimate an associated biodiffusion coefficient. To this end, we employed the analytical solution by Smith *et al.* (1987):

$$C(z) = C_0 \exp\left[- \sqrt{\frac{\lambda}{D_{fit}}} z \right] \tag{18}$$

with C_0 is the concentration of tracer at $z = 0$ and D_{fit} the diffusion coefficient that fits the data. The following fitting procedure was adopted: (i) to simulate core sectioning, a model-generated profile was "sliced" into 25 layers of 1 cm, which then produced an artificial data profile; (ii) a nonlinear regression of the form $y = a \exp(-bx)$ was performed on this artificial data profile; (iii) *Dfit* was calculated from the regression coefficient b as $Dfit = \lambda/b^2$ [note that because of the normalization of tracer profiles, the regression coefficient a was always equal to 1 as it corresponds to the parameter C_0 in Eq.(18)]. (iv) The sum of squared errors (SSE) provides an estimate of the quality of the

model fit, and this way, one can assess how strongly the profiles generated by patchy reworking deviate from a diffusive shape.

ii. Scenario B: effects of biological variability. The influence of biological variability in the ingestion rate was assessed by comparing two situations. (i) The sediment is completely reworked, but divided into n types of patches where tubificids have a different ingestion rate $k_{ing,i}^{\max}$ ($\alpha_b = 1$, n = 100). The n values for $k_{ing,i}^{\max}$ were assigned following the procedure described in Section 3a (ii) The sediment was completely reworked, and only a single type of tubificid was active ($\alpha_b = 1$, n = 1). In both cases, the downward migration of a pulse input of tracer was monitored at 10 d.

iii. Scenario C: the combination of patchiness and biological variability. To investigate the combined effect of patchiness and varying bioturbation activity within patches, simulations with n = 2, n = 10 and n = 100 were carried out. In all these simulations, the reworked fraction of the sediment surface was set to $\alpha_b = 0.75$. The values for the ingestion rates $k_{ing,i}^{\max}$ were assigned following the procedure described in Section 3a (Table 1). As in scenario A, two different boundary conditions were investigated: (C1) A pulse input flux of luminophores, with profiles at 10, 50 and 100 d. (C2). A constant external input flux of ^{234}Th and ^{210}Pb, with profiles toward the steady state.

4. Results

a. Effects of patchiness (Scenario A)

i. Scenario A1: A pulse input of luminophores. Tracer profiles for the pulse input were first simulated for the two end-member cases where $\alpha_b = 0$ and $\alpha_b = 1$ (Fig. 2). With $\alpha_b = 0$, the model reduces to the standard diffusion model with diffusion coefficient D_{nb}. As required, the simulated profiles match the analytical solution $C(t) = (1/\sqrt{\pi D_{nb} t})\exp(-z^2/(4D_{nb}t))$ of the diffusion model (Fig. 2a). With $\alpha_b = 1$ (Fig. 2e), the model produces the tracer profiles of the classical conveyor-belt model (Fisher *et al.,* 1980; Rice, 1986; Delmotte *et al.,* 2007). These profiles have two main features: (i) The pulse input is buried by bio-advection which generates a subsurface concentration peak that progressively migrates downward. Biodiffusion smears this peak, while particle ingestion at depth finally destroys it. (ii) From the surface to the peak maximum, concentrations are constant. This homogeneous layer results from the egestion of particles, which are immediately buried after their deposition at the SWI. The interplay of bio-advection and particle ingestion at depth makes concentrations quasi-homogeneous at 100 d. So given a characteristic depth of 5 cm and an induced bio-advective velocity of 50 cm yr^{-1}, sediment particles experience, on average, 10 ingestion-egestion cycles each year. In other words, the tracer pulse is uniformly homogenized throughout the mixed zone after about three ingestion-egestion cycles ($\sim$ 100 days).

A patchy distribution generates distinct tracer profiles (Fig. 2b–d) that combine features of the two end-member models. The exponential decrease near the surface, as in the

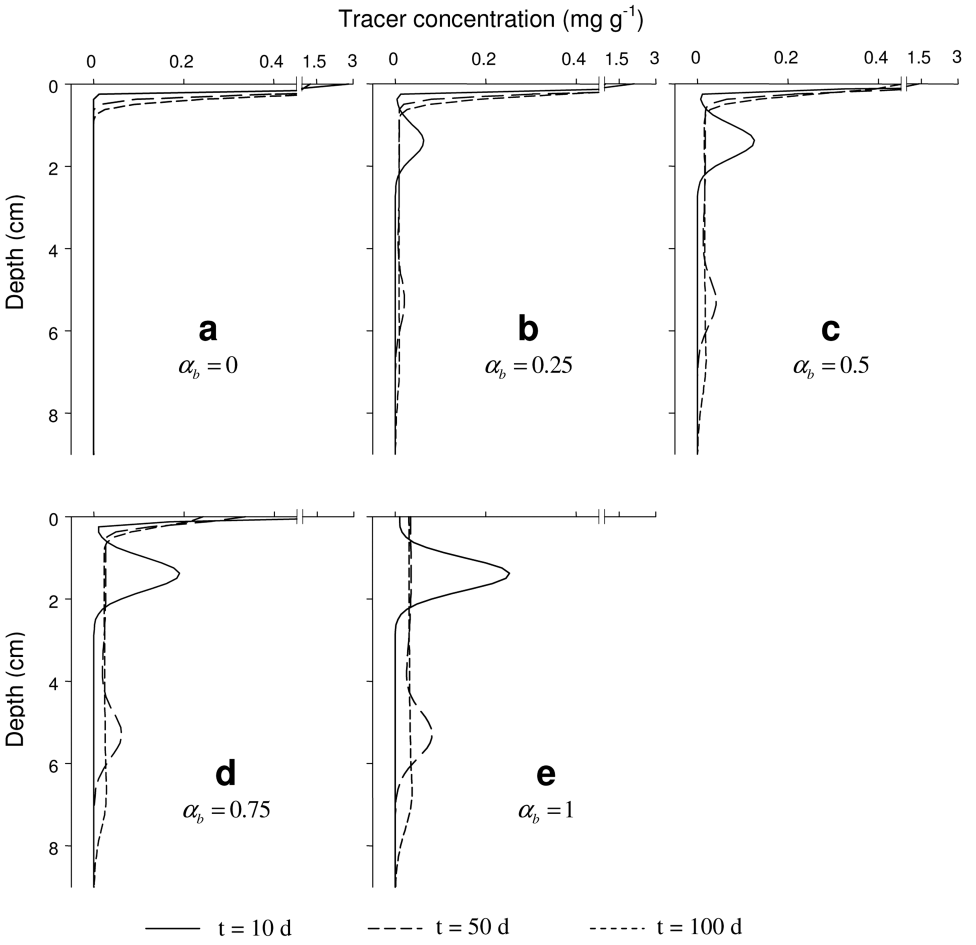

Figure 2. Tracer profiles resulting from the simulation scenario A1, which models the effect of patchiness on the pulse input of luminophores at the SWI. The patch ratio α_b denotes the fraction of the sediment area that is bioturbated (α_b takes the values 0, 0.25, 0.5, 0.75 and 1). When $\alpha_b = 0$, the model reduces to the abiotic diffusion model. When $\alpha_b = 1$, the model becomes the conventional conveyor-belt model. Between these two end-member values, the profiles result from the averaging of tracer transport in bioturbated and nonbioturbated patches. Dynamic simulations are carried out over time periods of 10, 50 and 100 days.

diffusion profiles, results from tracer that was deposited on the nonbioturbated patches. Simultaneously, the profiles also show the downward migration of a subsurface tracer peak, like in the profiles generated by conveyor-belt transport. At 100 d, the profiles exhibit an exponential decrease of concentrations near the surface and a quasi-homogeneous distribution of tracer from 1 down to 7 cm (the deeper limit of the ingestion zone). When the fraction of bioturbated surface area increases, the amplitude of the subsurface peak

Table 2. Estimation of biodiffusion coefficients (D_{fit}) from radio-tracer profiles generated by the deposit-feeding model, obtained via inverse modelling. The biodiffusion model [Eq. (18)] was applied to the radioisotope profiles obtained in scenario A2. Nonlinear regression was applied to provide the best fit. SSE means Sum of Squared Error, and represents the goodness of fit.

	^{234}Th		^{210}Pb	
α_b	D_{fit}	SSE	D_{fit}	SSE
0	0.098	1.2E-18	0.095	5E-05
0.25	0.45	8.7E-05	0.13	7.5E-03
0.5	0.75	7.4E-04	0.23	4.8E-02
0.75	1.53	5.6E-03	0.79	1.2E-01
1	136.7	4.9E-02	5.37	1.7E00

increases, and the concentration within the homogenized layer is higher at 100 d (more tracer is transferred to depth).

ii. Scenario A2: A constant input flux of ^{234Th} and ^{210}Pb. With no bioturbation ($\alpha_b = 0$), the simulated steady-state profiles of ^{234}Th and ^{210}Pb match the exponential decay predicted by the analytical solution [Eq. (18)]. This confirms the accuracy of our numerical integration routine (SSE of 10^{-18} and 10^{-5} in Table 2). The ^{234}Th activity vanishes within in the first millimeters, whereas ^{210}Pb reaches 10 cm, reflecting the different half-lives of these radio-tracers. When bioturbation covers the whole area ($\alpha_b = 1$), the two radio-tracers also generate a different response. ^{234}Th activity shows a quasi-linear decrease down to 8 cm, after which the activity becomes constant. In contrast, ^{210}Pb is homogenized from the surface down to 10 cm. Below 10 cm, where the ingestion zone stops, and bioadvection and biodiffusion cease, the profile adopts an exponentially decreasing shape.

When the sediment is patchily bioturbated ($0 < \alpha_b < 1$), ^{234}Th profiles show a strong decrease in activity in the first millimeters, as in the simulation with $\alpha_b = 0$, followed by a section of 6 cm where activity is low (Fig. 3b–d). ^{210}Pb profiles show a first exponential decrease from the surface to 10 cm, and a second exponential decrease from 10 to 20 cm which becomes more apparent with the increase of α_b. Even if the ^{234}Th and ^{210}Pb profiles show a exponential decrease, the activity of radioisotopes at depth is higher than required by the analytical solution of the diffusive model [Eq. (18)], especially with ^{210}Pb profiles which is more sensitive to the effect of conveying combined with the influence of the nonmixed layer within the bioturbated patches. Indeed, the absence of conveying below 10 cm within the bioturbated patches causes the accumulation of bio-advected tracer above this limit.

Activity at depth, resulting from the rapid transport of particles within the bioturbated patches, increases with an increase in the fraction of the surface that is bioturbated. As in scenario A1, an increase in the surface area of the bioturbated zone induces an increase of the amount of particles transferred to depth under a range of transport rates.

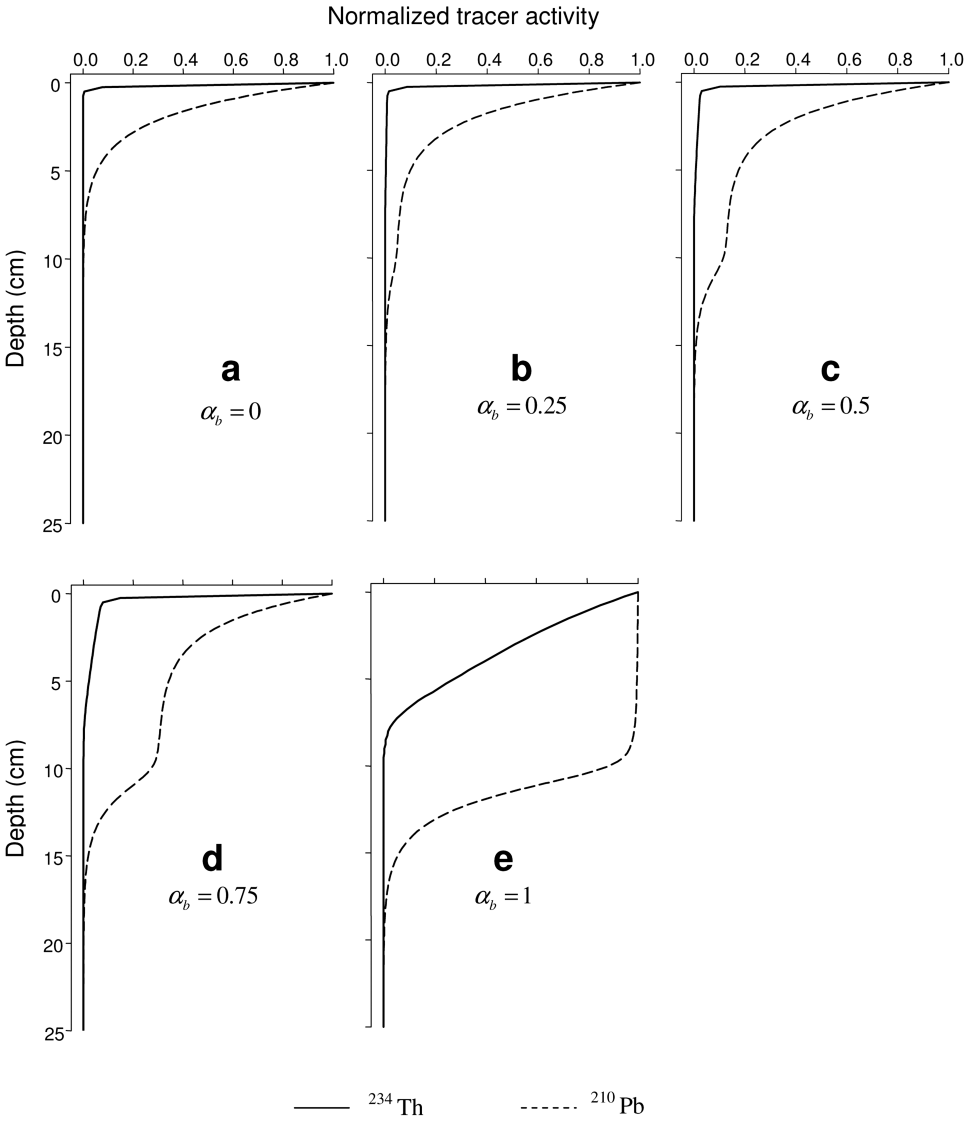

Figure 3. Tracer profiles resulting from the simulation scenario A2, which models the effects of patchiness on the constant supply of particle-bound radioisotopes at the SWI. ^{234}Th ($t_{1/2}$ = 24.1 d) and ^{210}Pb ($t_{1/2}$ = 22.3 yr) were simulated. The patch ratio α_b takes the values of 0, 0.25, 0.5, 0.75 and 1 (see also Fig. 2). Simulations were carried out until steady-state was reached.

The biodiffusive model [Eq. (18)] provides a poorer fit to the ^{210}Pb profiles than to the ^{234}Th profiles. The quality of the fit for both the tracers decreases when the bioturbated area increases, and ^{210}Pb profiles become totally nondiffusive when conveyor-belt transport occurs on the whole area (Table 2). Note also the high value of the biodiffusive coefficient

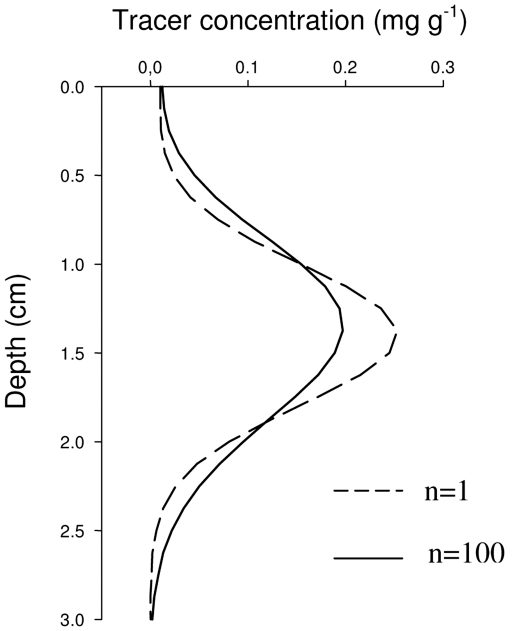

Figure 4. Tracer profiles resulting from the simulation scenario B. This scenario examines the effects of biological variability on a pulse input of luminophores at the SWI. The complete sediment surface is bioturbated ($\alpha_b = 1$). The quantity n represents the number of patches with a different type of organisms (different ingestion rates). Simulation output is shown for n = 1 (no diversity) and n = 100 (large diversity) after 10 days. When the variability increases, the subsurface peak broadens, which is conventionally interpreted as a biodiffusive process.

(136.7 $cm^2\ yr^{-1}$) needed to simulate the distribution of ^{234}Th in the presence of conveyor-belt transport over the total area. D_{fit} is always higher with ^{234}Th than with ^{210}Pb for a given value of α_b.

b. The effects of biological variability (Scenario B)

As required by the condition $\alpha_b = 1$, all the input pulse of tracer is buried as one subsurface peak, both in the cases with n = 1 and n = 100 (Fig. 4). The subsurface peaks of tracer are centred on the same depth in the two cases. The broadening of the peak is more pronounced with n = 100 than with n = 1, while the height of the peak is lower. With n = 1, all the particles move at the same velocity (about 50 $cm\ yr^{-1}$ at z = 0), even if they disperse around the peak of tracer by diffusion. Conversely, with n = 100, particles in the different patches migrates at different velocities (from 20 $cm\ yr^{-1}$ to 90 $cm\ yr^{-1}$). Hence, some particles are buried more rapidly and others more slowly than when all the patches feature the same ingestion rate. However, the Gaussian distribution of ingestion rates that we adopted is symmetric with a mean $\langle k_{ing}^{max} \rangle = 10\ yr^{-1}$. This implies that the tracer quantity that migrates more quickly than the mean equals to the tracer quantity that

migrates more slowly. Accordingly, the averaged bio-advective velocity will be the same as in the case with no biological variability (n = 1).

c. The effects of the combination of patchiness and biological variability (Scenario C)

i. Scenario C1: the luminophores case. First, as in the scenario A1, all the profiles adopt both the features of a diffusion profile (exponentially decreasing concentrations near the surface) and of a profile induced by conveyor-belt transport (subsurface peak(s) of tracer) (Fig. 5). Deceptively, the profiles from the simulations with n = 1, 2, 10 and 100 do not differ a great deal from each others. Particularly, the presence of several patches featuring different ingestion rates does not generate a clear signal of multiple subsurface peaks. Instead it just makes a more pronounced broadening of the peak of tracer at depth, as noticed in scenario C.

ii. Scenario C2: the case of a constant input flux of ^{234}Th and ^{210}Pb at the SWI. Adding variability in the ingestion rates does not change the profiles generated by patchy reworking, that are the same with n = 1, 2, 10 and 100 (Fig. 6).

5. Discussion

a. Existing patch models of bioturbation

The model presented here explicitly accounts for patchiness in bioturbation activity. In the past, some model approaches have accounted for the horizontal distribution of bioturbators, though have not explicitly investigated the issue in depth.

(i) Mohanty *et al.* (1998) presented a similar approach to ours, using the "average" of two separate solutions for bioturbated and nonbioturbated sediments. The model was used to examine the effect of oligochaete bioturbation on the flux of a soluble contaminant to the overlying water column. The bioturbated patches were assumed to be completely homogenized in the vertical (i.e. uniform concentration with depth) and the contaminant flux was obtained by surface renewal theory. The nonbioturbated patches were modeled by a simple diffusion equation. Our approach can be viewed as a generalization of the model presented by Mohanty *et al.* (1998). Rather than adopting the simplifying assumption of complete homogenization, we employ an explicit 1D model for the particle transport induced by oligochaetes bioturbation.

(ii) François *et al.* (1997, 2001, 2002) developed a two-dimensional (2D) model of the sediment (horizontal and vertical dimensions), where they designated specific areas bioturbated and nonbioturbated. Different functional groups of organisms were included, which generated a different mode of transport within bioturbated zones. The bioturbated zones remained static over time, and no exchange was assumed between bioturbated and nonbioturbated zones. The 2D model itself was set up as a discrete, matrix model, where sets of neighboring grid cells were designated as bioturbated zones, the flow of material between these cells was suitably parameterized. Our model is a one-dimensional, continu-

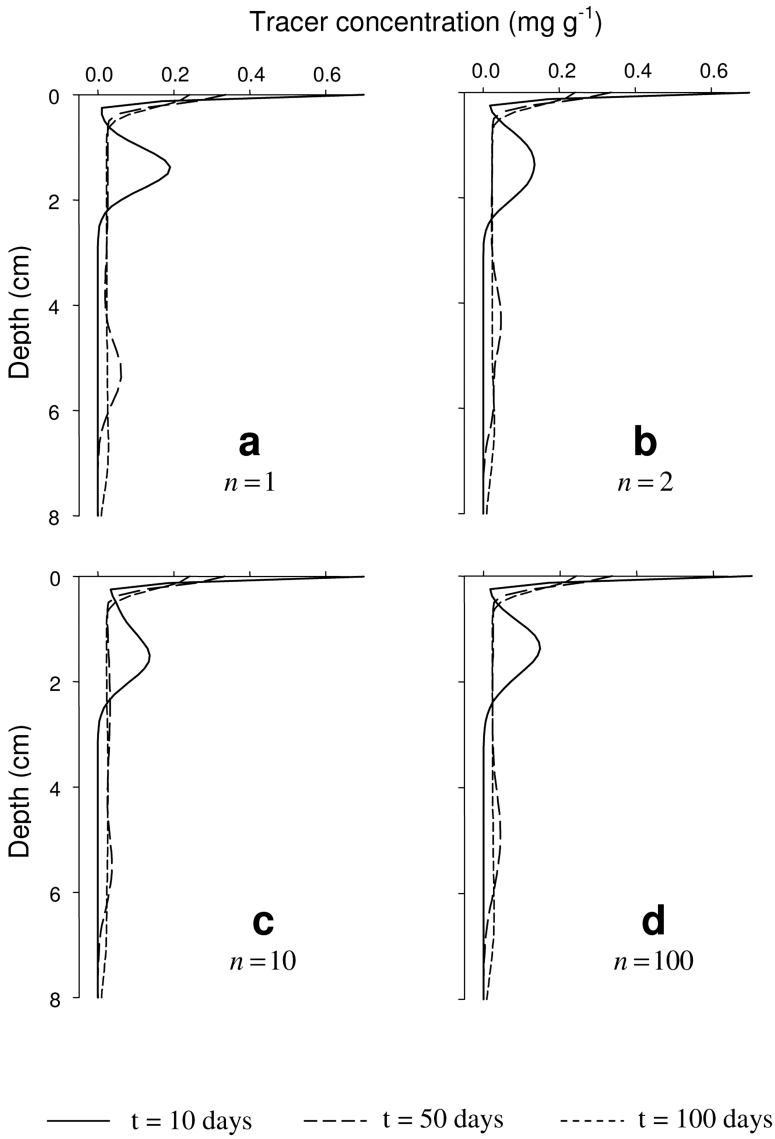

Figure 5. Tracer profiles resulting from the simulation scenario C1. This scenario combines the effects of patchiness and biological variability on a pulse input of luminophores at the SWI. In this scenario, α_b takes the value 0.75, and the number of patches (each populated by an organism with a different ingestion rate) is set to n = 1, 2, 10 and 100. The ingestion rate within an individual patch is drawn from a Gaussian distribution with mean ingestion rate 10 yr^{-1}. Descriptive statistics of the ingestion rate distribution are given in Table 1.

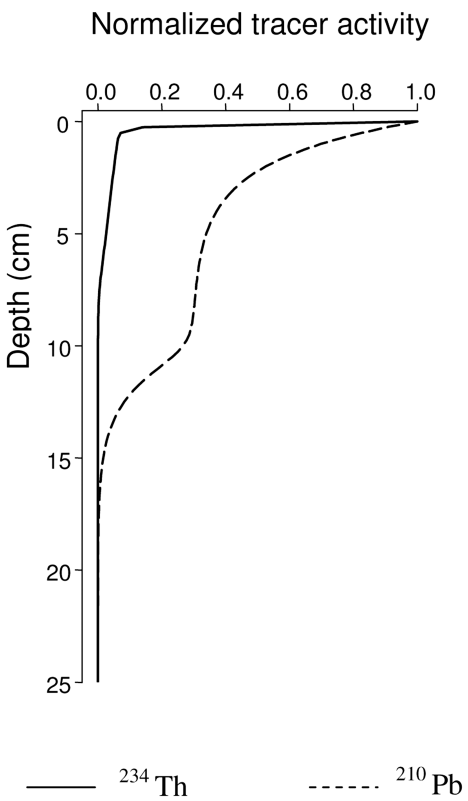

Figure 6. Tracer profiles resulting from the simulation scenario C2, which describes the combined effects of patchiness and biological variability on a constant supply of particle-bound radioisotopes at the SWI. The tracers ^{234}Th ($t_{1/2}$ = 24.1 d) and ^{210}Pb ($t_{1/2}$ = 22.3 yr) were simulated. In this scenario, the values for α_b and n are the same as in Figure 5. Simulations were carried out towards the steady-state. Because the tracer profiles are nearly identical for n = 1, 2, 10 and 100 (no effect of biological variability), only one profile is represented for each tracer.

ous counterpart of the 2D model by François and co-workers. We also assume that patches remain static in time and that no exchanges occur between bioturbated and nonbioturbated zones. Our 1D model strongly simplifies the 2D approach of the François *et al.,* but retains its principal advantage: the possibility to include distinct modes of bioturbation within different patches. As shown by Meysman *et al.* (2003), discrete matrix models model exactly the same process as their continuous counterparts. The latter though have several advantages in terms of model analysis. One problem with matrix transition models (and especially with 2D versions) is the rapid inflation of free parameters: suitable transport coefficients need to be declared for the exchange between every pair of grid cells. Continuous models contain significantly fewer free parameters, and are computational far more efficient, which is a strong advantage for model analysis.

(iii) The Lattice-Automaton Bioturbation Simulator (LABS) involves a very different form, and comprises a virtual sediment environment in which bioturbation experiments can be simulated (Boudreau *et al.,* 2001; Reed *et al.,* 2006; Huang *et al.,* 2007). Automaton organisms are programmed with a certain behavior (movement, feeding, etc), and the activity of these automatons then generates a certain mode of particle displacement. The main purpose of LABS is not to fit tracer data like classical bioturbation models, but to run virtual mixing simulations to investigate how microscopic particle dispersal leads to the macroscopic patterns (e.g. diffusive behavior). Until now, only homogeneous mixing simulations have been carried out in LABs, where random deposit feeders have access to all parts of the sediment. However, the LABs environment would represent a suitable laboratory to complement the present analysis of patchiness. Accordingly, simulations of heterogeneous, patchy reworking would clearly be a valuable direction for future research in LABS.

(iv) Recently, a new continuous 1D model formulation has been proposed for bioturbation, based on the continuous-time random walk formalism (Meysman *et al.,* 2008 a, b). This model explicitly accounts for the fact that particle can have variable "waiting time" and "step length" behavior in consecutive bioturbation events. This CTRW model does not explicitly include spatial patterns of bioturbation, but is able to account for this indirectly: horizontal heterogeneity is translated into vertical stochasticity of particle motion. For example, in nonbioturbated patches, mixing events are scarce (long waiting times), and step lengths are typically small. In contrast, in bioturbated patches, mixing events are more frequent, and particle may be dislocated over longer distances. In the CTRW model, these two modes of transport can be condensed to an "average" bioturbation fingerprint, which will consist of a bimodal step length and waiting time probability distribution. Recently, the CTRW model has been successfully applied to the patchy reworking of bivalves in laboratory microcosms (Maire *et al.,* 2007). Accordingly, one suggestion for future work is to investigate how "averaged" continuous 1D models (as developed here) can be mapped onto equivalent CTRW descriptions, thus providing a mechanistic explanation for the "empirical" stochasticity incorporated in CTRW models.

b. Tracer dependence of biodiffusion

Our simulation results provide two revealing insights on the relation between head-down deposit feeding and the biodiffusion model. Foremost, the nonlocal mode of particle reworking induced by the head-down deposit feeding of oligochaetes strongly deviates from the local, symmetric and small-scale mixing that is usually associated with biodiffusion. As a result, one expects the biodiffusion model to perform poorly for tracer profiles generated by head-down deposit feeding. This is also generally the case: as the bioturbated area increases, the goodness of fit of the biodiffusion model decreases (based on the sum of squared errors—see Table 2). However, this deviation from diffusive behavior is markedly dependent on the tracer: the fit to the ^{234}Th profiles (half-life 24.1 days) is consistently better than to the ^{210}Pb profiles (half-life 22.3 years). This is also corroborated by the shape

of the profiles: the ^{234}Th profiles display more closely resemble "exponentially decreasing" shape, as would be expected from the solution of the biodiffusion model. This result can be explained by the cycling frequency of radio-isotope particles, i.e., the average number of times that particles will go through the process of ingestion at depth followed by egestion at the surface. The cycling frequency can be calculated as the ratio between the flux of egested material F_{eg} [Eq. (14)] and the external entering flux of particles F_{ext}. In the case of ^{234}Th, particles experience on average 0.59 cycles of ingestion-egestion, and so the radiotracer particles mostly decays before reaching the depth of ingestion. In contrast, ^{210}Pb coated particles will undergo about 220 ingestion-egestion cycles, reflecting the long half-life of ^{210}Pb. Cycling homogenizes the tracer within the mixed zone, thus explaining the "vertical" character of the ^{210}Pb profiles. Overall, the ingestion term in Eq. (1) has a much greater influence on ^{210}Pb than ^{234}Th profiles. Without the ingestion term, Eq. (1) turns into a classical advection-diffusion equation. So when the ingestion becomes important, the shape of tracer profiles will markedly differ from the one expected by diffusion or advection-diffusion. Clearly, the goodness of fit of the biodiffusive model cannot be considered as a good criterion to determine whether transport is local or nonlocal. For both ^{234}Th and ^{210}Pb, the underlying transport mechanism is identical, but the goodness of fit is very different.

A second remarkable observation is that the estimated biodiffusion coefficients D_{fit} are systematically higher for ^{234}Th as compared to ^{210}Pb. The ratio of ^{234}Th/^{210}Pb values also increases when the bioturbated area increases, indicating that the tracer dependence results from the biological transport. This tracer dependence of biodiffusion coefficients is currently a hotly debated topic in bioturbation research. It has been observed in studies where short-lived and long-lived tracer profiles are analyzed from the same environment (Smith *et al.,* 1993). Moreover, global database analysis of biodiffusion coefficients show a systematic bias towards higher values for the ^{234}Th method when compared to values obtained from the ^{210}Pb method (Middelburg *et al.,* 1997).

To date, two contrasting explanations have been proposed to explain this tracer dependence. In one perspective, the hypothesis of age-dependent mixing, the tracer-dependence is real, meaning that ^{234}Th particles are mixed differently (i.e. with a higher mixing intensity) than ^{210}Pb particles. Age-dependent mixing proposes that short-lived radioisotopes are principally associated with fresh and labile particles, which are preferably ingested by organisms, and hence, mixed at higher rates (Smith *et al.,* 1993). In a second alternative view, the tracer-dependence is considered as a modeling artefact, resulting from the fact that the biodiffusion model is not applicable at short time scales. Meysman *et al.* (2003) already noted that the applicability of the biodiffusion model depends on the half-life of the tracer: for short-lived isotopes the assumptions of the biodiffusion model are likely to be violated. In subsequent work based on LABS simulations, Reed *et al.* (2006) showed that the tracer dependence of biodiffusion coefficients can indeed arise as a model artefact. For short-lived radioisotopes, the number of bioturbation events that takes place before the tracer decays is insufficient. This

generates D_b values that are biased toward high values. Our simulations here support this idea that the tracer-dependence of biodiffusion coefficient results from a modeling artefact. In the simulations of Figure 3, the ^{234}Th particles and the ^{210}Pb particles experience exactly same particle transport. Still the resulting D_{fit} values differ by two orders of magnitude (137 cm^2 yr^{-1} for ^{234}Th compared to 5 cm^2 yr^{-1} for $\alpha_b = 1$ in Table 2). Our results emphasize that one should be cautious when applying the biodiffusion model to analyze data profiles of short-lived tracers.

c. Patchiness and the interpretation of tracer profiles

As can be seen from Figures 2 and 3, the effect of patchiness is to create "averaged" profiles that include both features of bioturbated and nonbioturbated zones. The tracer profiles in a patchy reworked area are different in shape from the fully bioturbated site. In the case of the luminophores, the patchy reworked core displays a subsurface peak at depth together with exponentially decreasing tracer concentrations in the uppermost sediment layer. This tracer decreases in the uppermost sediment layer is due to abiotic mixing in the nonbioturbated patches. In the fully reworked core, this surface gradient is not present, and there is only a subsurface peak. Similarly, the ^{210}Pb profiles in the patchy reworked core display a gradually decreasing tracer concentration near the surface, together with accumulation of tracer at depth. In the fully reworked core, the upper layer has a very different profile, which shows no tracer gradient.

Note that the "blended" nature of the tracer profiles in patchily reworked cores could easily lead to a misinterpretation of the mechanisms governing particle transport. Here, the tracer profiles in the patchy cores could be easily—though mistakenly—attributed to deposit feeders that act as downward conveyers. These organisms collect material at the surface (which causes mixing in the surface layer). Subsequently, they drag this material into their burrows and deposit this at depth (generating subsurface peaks in luminophore profiles or accumulation at depth of radiotracers). Typical examples of such profiles were found by Smith *et al.* (1986) with the large marine worm *Sipunculida* that ingests sediment at the surface and egests this material at depth, or for the polychaete *Nereis diversicolor* that drags down surface particles in its galleries (François *et al.,* 2002; Fernandes *et al.,* 2006; Duport *et al.,* 2006). Here however, exactly the same profiles are created by entirely different mechanism of deposit-feeding by tubificids: head-down deposit feeding (i.e. moving particles up) instead of downward conveying (i.e. dragging particles down). As a consequence, one should be careful when deducing the actual feeding or bioturbation mode from tracer profiles shapes. The shape of the profile in itself is not conclusive: both animal behavior and mixing mechanism should be known (Reed *et al.,* 2006), and as shown here, lateral heterogeneity in bioturbation should be assessed in addition.

d. Intra-population variability in bioturbation rates

In addition to the effects of patchiness, we have examined the effect of biological variability on bioturbation activity. This was done by "equipping" n patches with different

parameters in the conveyor-belt model. Our original intention was to examine the effects of intra-population variability, where each patch represented an individual or a size-class of the same bioturbating organism. However, in an alternative view, one can also imagine a mixed community of different head-down deposit feeders, where each separate patch is now inhabited by a different species (inter-population variability). Note that in existing conveyor-belt models, authors have already accounted for biological variability in one specific way. In the standard formulation, the ingestion rate is made dependent on depth, as represented by a Gaussian ingestion function centred around an average ingestion depth (Fisher *et al.,* 1980; Robbins, 1986; Delmotte *et al.,* 2007). This formulation can be mechanistically justified if one assumes that the distribution of the organism size follows a Gaussian distribution, and that the feeding depth linearly scales with the size of organisms.

Here we have introduced a second type of intra-population variability, assuming that the feeding activity will also vary between individuals, and so we varied the ingestion rate between patches. This variability in the ingestion rate is also described with a Gaussian function, being the standard representation of biological phenomena. Overall, our results show that the inclusion of intra-population variability in the ingestion rate does not strongly affect the shape of the resulting tracer profiles. In the case of a constant input flux of radioisotopes, the differences in the profiles were very marginal. In the case of short-term experiments with luminophores, intra-population variability in the ingestion rates does show an effect, causing the broadening of the subsurface tracer peaks. Such peak broadening has been experimentally documented in luminophore pulse-tracer experiments with conveyor-belt deposit feeders (Ciutat *et al.,* 2005a, b). This peak broadening is conventionally interpreted and modeled as a biodiffusive process (Robbins, 1986; Delmotte *et al.,* 2007). The present work however shows that inherent variability in ingestion rates can be the underlying mechanism of such peak broadening. In other words, variability in bio-advective velocities makes that tracer profiles look more diffusive. This means that what we conventionally interpret as a small-scale vertical mixing could equally result from the horizontal averaging of adjacent nonlocal mixing activity, a mechanism that has been theoretically forwarded in Meysman *et al.* (2003).

e. Patchiness, temporal and spatial scales

Clearly, a key question is when it is truly necessary or useful to account for patchiness in bioturbation models? In the past, 1D formulations that do not account for patchiness have been quite successful in modeling tracer profiles. This indicates that patchiness must not necessarily be a component of bioturbation models. In theory, this can be due either one of two reasons: (1) sediments are homogeneously bioturbated on the spatial scale of the core, and so patchiness is not an important aspect of bioturbation under natural conditions, or (2) the sediment is reworked in patches, but the time scale of observation is sufficiently long, so that organisms have moved horizontally and the whole area is reworked.

We believe the second option most closely corresponds to the actual process of bioturbation in natural environments. Recently, the patchy nature of bioturbation, has been

demonstrated, mostly because of the emergence of new 2D tracer techniques based on image analysis (Gilbert *et al.,* 2003; Solan *et al.,* 2004; Maire *et al.,* 2007). 2D monitoring of fluorescent tracers deposited at the sediment-water interface clearly shows that particle redistribution is patchy at the spatial scale of a sediment core and over the time scale of few days. Maire *et al.* (2007) showed that the bivalve *Abra ovata* creates conical mixed zones as a result of siphon movement when scanning the sediment surface for food particles. After some time, the bivalve dislocates to another (not-yet-bioturbated) location and creates a new conical mixed zone. Similarly, freshwater tubificid oligochaetes (*Tubifex sp.*), the patchy nature of their reworking activity was already shown in Figure 1. Even with a high density (50 000 ind.m^{-2}), the reworked area remains patchy after considerable time (11 days), which presumably results from the aggregative behavior of these worms. These two examples show that the spatial and temporal characteristics of patchiness are obviously influenced by the specific feeding behavior and traits of the organisms involved. Clearly, one can distinguish slow movers, which will establish stable patches that remain for quite long times, and fast movers, which rapidly dislocate and establish new patches elsewhere.

This aspect of time scale is well illustrated by following model, which describes how sediments are progressively bioturbated (Fig. 7). Initially, the organisms will only rework a certain part of the sediment area (one or more patches). However, as time progresses, organisms will dislocate, and so, new sections of the sediment will be bioturbated, while other sections are abandoned. We distinguish three types of sediment: sediment that is currently reworked (black area), sediment that has never been reworked (gray area), and sediment that is currently not reworked, but has been reworked in the past (hatched area). The fraction α_b introduced previously denotes the sediment area that is currently reworked (black area/total area). If we assume that the area that is colonized per unit of time exactly matches the area that is abandoned per unit of time, this fraction α_b does not change over time. We also introduce the fraction $\beta_b(t)$, which denotes the total sediment area that has been reworked over time (that is the sum of black and hatched areas). Now if we think of the colonization of sediment are sections as a Poisson process, where each section has an equal chance of being newly colonized, the time evolution of the total reworked area becomes (Maire *et al.,* 2007):

$$\beta_b(t) = \alpha_b + (1 - \alpha_b)(1 - \exp(-t/t_\alpha)) \tag{19}$$

The time t_α provides a characteristic time scale over which organism will dislocate and colonize new portions of sediment. For sufficiently long times $t \ll t_\alpha$, the whole sediment area will eventually become bioturbated ($\beta_b = 1$). Slow movers are associated with large values for t_α, fast movers have small values for t_α. In laboratory microcosms containing the bivalve *Abra ovata,* Maire *et al.* (2007) monitored the evolution of β_b with time using the 2D image analysis techniques. These authors found that the above model equation adequately described the evolution of the reworked surface area, and obtained values for t_α varying between 0.5 to 35 days.

Accordingly, the question whether one should account for patchiness requires a

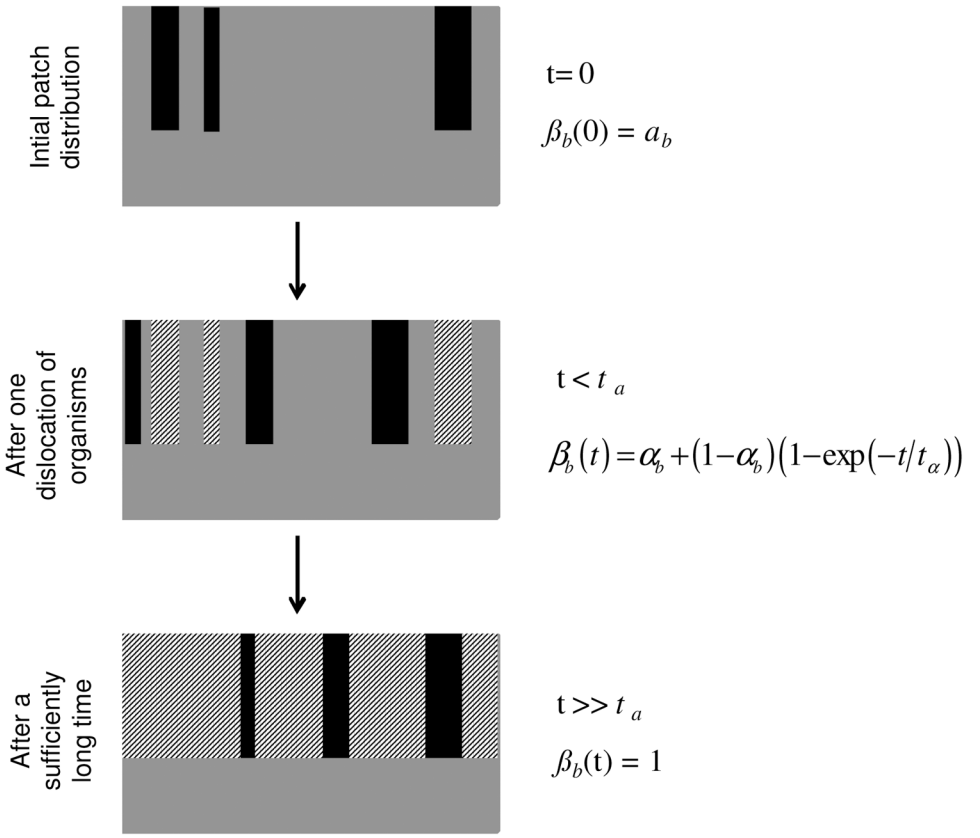

Figure 7. Conceptual scheme of the temporal dynamics of patchy sediment reworking. Three types of sediment are distinguished: sediment that is currently reworked (black area), sediment that has never been reworked (gray area), and sediment that is currently not reworked, but has been reworked in the past (hatched area). Eq. (19) describes the total area fraction $\beta_b(t)$ that has been reworked over time, i.e. the sum of the area that is currently bioturbated (α_b) and the area that has been reworked in the past. Animals dislocate and colonize new patches, following a Poisson process: α_b remains constant whereas β_b increases. After a sufficient long time, the whole sediment area is reworked and $\beta_b = 1$. The time scale over which sediment becomes s completely reworked depends on the characteristic time scale t_α over which animals colonize new patches.

comparison of two time scales: the time scale of observation (~ half-life of the tracer) versus the time scale of which the whole sediment becomes bioturbated (~ the characteristic time scale t_α of lateral mobility of the organisms). When the time scale of observation is sufficiently larger than the time scale of lateral mobility, the issue of patchiness at the spatial scale of the core can be ignored. In other words, for long-lived radiotracers, the effects of lateral patchiness are "averaged away" and classical non-patchy bioturbation models will do fine. However, for short time-scale experiments (as with luminophores and short-lived radio nuclides), we believe that patchi-

ness is an important, and presently overlooked issue. At present we do not have a very good dataset on the lateral mobility times of t_α of natural communities. This is clearly an important topic that should be addressed in future research. However, based on the Maire *et al.* (2007) values (0.5–35 days for intensely mixed sediments) and the presence of patchiness after tens of days in the experiments of Ciutat (Fig.1), we hypothesize that t_α values might be similar to the time scales typically adopted in luminophores and short-lived radio nuclides methods.

Accordingly, when analyzing the tracer profiles that result from short-time scale experiments, one should be careful with respect to the type of models that are used and cautious about assumptions that underlie these models (e.g. steady state, biodiffusion). Note that related problems with short-time scale methods were brought up in the above discussion of the issue of tracer dependence of biodiffusion coefficients. Overall, short-time scale bioturbation experiments emerge as methods that generate data which are challenging and difficult to interpret. Our results thus corroborate recent findings that question the validity and applicability of traditional bioturbation models for tracer data derived from short-time scale experiments (Meysman *et al.,* 2003, 2008a; Reed *et al.,* 2006).

6. Conclusion

Up to now, patchiness of organism distribution and biological variability in transport rates within a population have scarcely been accounted for in the modeling studies of bioturbation, mostly because the conventional 1D models successfully represented the measured profiles. In this paper, we propose a general model that includes these components, but keeps a relatively simple mathematical formulation: the model is vertically 1D, and only one additional parameter is included to represent patchiness. Analysis of the model showed great influence of patchiness on final tracer distribution, whatever the type of tracer (luminophores, short- and long-lived radiotracers). Variations in transport rates within a population of bioturbators do not highly influence resulting profiles, but generate biodiffusive-like profiles. This modeling tool should be useful to better interpret tracer profiles and to better understand the influence of organism density and patchiness on sediment mixing. Its application to real data is clearly needed to assess its accuracy and its ease of use. The next step would be to develop a transient-patch model of bioturbation to explore the effects of patch migration over long time scales.

Acknowledgments. We gratefully thank Pete Jumars for his help and constructive comments, and an anonymous reviewer for stimulating criticism. We also thank Bob Aller for his helpful comments and Aurelie Ciutat for kindly providing the picture of tubificid reworking. This research was financed by several GIS Ecobag mediated programmes: MATE, AEAG, Midi-Pyrenees Region, CNRS/PEVS, and European FEDER funds. Sebastien Delmotte benefited from a grant from theFrench Ministry of Research and Education (MESR). Filip Meysman was supported by an Odysseus grant from Research Foundation Flanders (FWO). This is publication 21 of the Nereis Park.

REFERENCES

Aller, R. C. 1982. The effects of macrobenthos on chemical properties of marine sediment and overlying water, *in* Animal-Sediment Relations, P. L. McCall and M. J. S. Tevesz, eds., Plenum, NY, 53–102.

Aller, R. C., L. K. Benninger and J. K. Cochran. 1980. Tracking particles-associated processes in nearshore environments by use of 234 Th/238U disequilibrium. Earth Planet. Sci. Lett., *47,* 161–178.

Aller, R. C. and R. E. Dodge. 1974. Animal-sediment relations in a tropical lagoon Discovery Bay, Jamaica. J. Mar. Res., *32,* 209–232.

Archer, D. E., J. L. Morford and S. R. Emerson. 2002. A model of suboxic sedimentary diagenesis suitable for automatic tuning and gridded global domains. Global Biogeochem. Cy., *16,* 1017, doi:10.1029/2000GB001288.

Berner, R. A. 1980. Early Diagenesis, A Theoretical Approach, Princeton Series in Geochemistry, Princeton University Press.

Boudreau, B. P. 1986a. Mathematics of tracer mixing in sediments: I. Spatially-dependent, diffusive mixing. Amer. J. Sci., *286,* 161–198.

—— 1986b. Mathematics of tracer mixing in sediments: II. Nonlocal mixing and biological conveyor-belt phenomena. Amer. J. Sci., *286,* 199–238.

—— 1997. Diagenetic Models and Their Implementation. Berlin, Springer.

Boudreau, B. P., J. Choi, F. J. R. Meysman and F. François-Carcaillet. 2001. Diffusion in a lattice-automaton model of bioturbation by small deposit-feeders. J. Mar. Res, *59,* 749–768.

Boudreau, B. P. and D. M. Imboden. 1987. Mathematics of tracer mixing in sediments: III. The theory of non-local mixing within sediments. Amer. J. Sci., *287,* 693–719.

Ciutat, A., P. Anschutz, M. Gerino, and A. Boudou. 2005a. Effects of bioturbation on cadmium transfer and distribution into freshwater sediments. Environ. Toxicol. Chem., *24,* 1048–1058.

Ciutat, A., M. Gerino, N. Mesmer-Dudons, P. Anschutz and A. Boudou. 2005b. Cadmium bioaccumulation in Tubificidae from the overlying water source and effects on bioturbation. Ecotoxicol. Environ. Safety, *60,* 237–246.

Commito, J. A., C. A. Currier, L. R. Kane, K. A. Reinsel and I. M. Ulm. 1995. Dispersal dynamics of the bivalve *Gemma gemma* in a patchy environment. Ecol. Mono., *65,* 1–20.

Delmotte, S., F. R. J. Meysman, A. Ciutat, S. Sauvage, A. Boudou and M. Gerino. 2007. Cadmium transport in sediments by tubificid bioturbation: an assessment of model complexity. Geochim. Cosmochim. Acta, *71,* 844–862.

Duport, E., G. Stora, P. Tremblay and F. Gilbert. 2006. Effects of population density on the sediment mixing induced by the gallery-diffusor *Hediste* (*Nereis*) *diversicolor,* O. F. Müller, 1776. J. Exp. Mar. Biol. Ecol., *336,* 33–41.

Fernandes, S., F. J. R. Meysman and P. Sobral. 2006. The influence of Cu contamination on *Nereis diversicolor* bioturbation. Mar. Chem., *102,* 148–158.

Fisher, J. B., W. J. Lick, P. L. McCall and J. A. Robbins. 1980. Vertical mixing of lake sediments by tubificid oligochaetes. J. Geophys. Res., *85,* 3997–4006.

François, F., M. Gerino, G. Stora, J. P. Durbec and J. C. Poggiale. 2002. Functional approach to sediment reworking by gallery-forming macrobenthic organisms: modeling and application with the polychaete Nereis diversicolor. Mar. Ecol. Prog. Ser., *229,* 127–136.

François, F., J. C. Poggiale., J. P. Durbec and G. Stora. 1997. A new approach for the modeling of sediment reworking induced by a macrobenthic community. Act. Biotheor., *45,* 295–319.

—— 2001. A new model of bioturbation for a functional approach to sediment reworking resulting from macrobenthic communities, *in* Organism-Sediment Iinteractions, J. Y. Aller, S. A. Woodin and R. C. Aller, eds., University of South Carolina, Columbia, The Belle W. Baruch Library in Marine Science, *21,* 73–86.

Gerino, M., R. C. Aller, C. Lee, J. K. Cochran, J. Y. Aller, M. A. Green and D. Hirschberg. 1998. Comparison of different tracers and methods used to quantify bioturbation during a spring bloom: ^{234}Thorium, luminophores and Chlorophyll *a.* Estuar. Coastal Shelf. Sci, *15,* 1483–1496.

Gilbert, F., S. Hulth, N. Stroemberg, K. Ringdahl and J. C. Poggiale. 2003. 2-D optical quantification of particle reworking activities in marine surface sediments. J. Exp. Mar. Biol. Ecol., *285/286,* 251–263

Goldberg, E. D. and M. Koide. 1962. Geochronological studies of deep-sea sediments by the Io/Th method. Geochim. Cosmochim. Acta, *26,* 417–450.

Gray, J. S. 1974. Animal sediment relationship. Oceanogr. Mar. Biol. Rev., *12,* 223–261.

Guinasso, N. L. and D. R. Schink. 1975. Quantitative estimates of biological mixing rates in abyssal sediments. J. Geoph. Res., *80,* 3032–3043.

Hewitt, J. E., R. D. Pridmore, S. F. Thrush and V. J. Cummings. 1997. Assessing the short-term stability of spatial patterns of macrobenthos in a dynamic estuarine system. Limnol. Oceanogr., *42,* 282–288.

Honkoop, P. J. C., G. B. Pearson, M. S. S. Lavaleye and T. Piersma. 2006. Spatial variation of the intertidal sediments and macrozoo-benthic assemblages along Eighty-mile Beach, North-western Australia. J. Sea Res., *55,* 278–291.

Huang, K., B. P. Boudreau and D. C. Reed. 2007. Simulated fiddler-crab sediment mixing. J. Mar. Res., *65,* 491–522.

Kneib, R. T. 1984. Faunal relationships in seagrass and marsh ecosystems, Estuaries, *4,* 392–412.

Levinton, J. and B. Kelaher. 2004. Opposing organizing forces of deposit-feeding marine communities. J. Exp. Mar. Biol. Ecol., *300,* 65–82.

Lindsay, S. M., D. S. Wethey and S. A. Woodin. 1996. Modeling interactions of browsing predation, infaunal activity, and recruitment in marine soft-sediment habitats. Am. Nat., *148,* 684–699.

Maire, O., J. C. Duchêne, A. Grémare, V. S. Malyuga and F. J. R. Meysman. 2007. A comparison of sediment reworking rates by the surface deposit-feeding bivalve *Abra ovata* during summertime and wintertime, with a comparison between two models of sediment reworking. J. Exp. Mar. Biol. Ecol., *343,* 21–36

Meysman, F. J. R., B. P. Boudreau and J. J. Middelburg. 2003. Relations between local, non-local, discrete and continuous models of bioturbation. J. Mar. Res., *61,* 391–410.

—— 2005. Modeling reactive transport in sediments subject to bioturbation and compaction. Geochim. Cosmochim. Acta, *69,* 3601–3617.

Meysman, F. J. R., V. S. Malyuga, B. P. Boudreau and J. J. Middelburg. 2008a. A generalized stochastic approach to particle dispersal in soils and sediments. Geochim. Cosmochim. Acta, *72,* 3460–3478.

—— 2008b. Quantifying particle dispersal in aquatic sediments at short time scales: What model should we use? Aq. Biol., *2,* 239–254.

Meysman, F. J. R., J. J. Middelburg and C. H. R. Heip. 2006. Bioturbation: a fresh look at Darwin's last idea. Trends. Ecol. Evol., *21,* 688–695.

Middelburg, J. J., K. Soetaert and P. M. J. Herman. 1997. Empirical relationships for use in global diagenetic models. Deep-Sea Res. I, *44,* 327–344.

Mohanty, S., D. D. Reible, K. T. Valsaraj and L. J. Thibodeaux. 1998. A physical model for the simulation of bioturbation and its comparison to experiments with oligochaetes. Estuaries, *21,* 255–262.

Parry, D. M., M. A. Kendall, D. A. Pilgrim and M. B. Jones. 2003. Identification of patch structure within marine benthic landscapes using a remotely operated vehicle. J. Exp. Mar. Biol. Ecol., *285/286,* 497–511.

Peterson, C. H. 1991. Interdital zonation of marine invertebrates in sand and mud. Am. Sci., *79,* 236–249.

Reed, D. C., K. Huang, B. P. Boudreau and F. J. R. Meysman. 2006. Steady-state tracer dynamics in a lattice-automaton model of bioturbation. Geochim. Cosmochim. Acta, *70,* 5855–5867.

Rice, D. L. 1986. Early diagenesis in bioadvective sediments: Relationships between the diagenesis of beryllium-7, sediment reworking rates, and the abundance of conveyor-belt deposit-feeders. J. Mar. Res., *44,* 149–184.

Robbins, J. A. 1986. A model for particle-selective transport of tracers in sediments with conveyor belt deposit feeders. J. Geophys. Res., *91,* 8542–8558.

Smith, C. R., R. H. Pope, D. J. DeMaster and L. Magaard. 1993. Age-dependent mixing of deep-sea sediments. Geochim. Cosmochim. Acta, *57,* 1473–1488.

Smith, J. N., B. P. Boudreau and V. Noshkin. 1986. Plutonium and ^{210}Pb distributions in northeast Atlantic sediments: subsurface anomalies caused by nonlocal mixing. Earth Planet. Sci. Lett., *81,* 15–28.

Solan, M., B. D. Wigham, I. R. Hudson, R. Kennedy, C. H. Coulon, K. Norling, H. C. Nilsson and R. Rosenberg. 2004. *In situ* quantification of bioturbation using time-lapse fluorescent sediment profile imaging (f-SPI), luminophore tracers and model simulation. Mar. Ecol. Prog. Ser., *271,* 1–12.

Thrush, S. F. 1991. Spatial patterns in soft-bottom communities. Trends Ecol. Evol., *6,* 75–79.

Thrush, S. F., V. J. Cummings, P. K. Dayton, R. Ford, J. Grant, J. E. Hewitt, A. H. Hines, S. M. Lawrie, R. D. Pridmore, P. Legendre, B. H. McArdle, D. C. Schneider, S. J. Turner, R. B. Whitlatch and M. R. Wilkinson. 1997. Matching the outcome of small-scale density manipulation experiments with larger scale patterns: an example of bivalve adult/juvenile interactions. J. Exp. Mar. Biol. Ecol., *216,* 153–169.

Timmermann, K., G. T. Banta, J. Larsen and O. Andersen. 2003. Modeling particle and solute transport in sediments inhabited by *Arenicola marina.* Effects of Pyrene on transport processes. Vie Milieu, *53,* 187–200.

Wheatcroft, R. A., P. A. Jumars, C. R. Smith and A. R. M. Nowell. 1990. A mechanistic view of the particulate biodiffusion coefficient: step lengths, rest period and transport directions. J. Mar. Res., *48,* 177–207.

Received: *14 January, 2008;* revised: *30 April, 2008.*